Proceedings World Geothermal Congress 2026
Calgary, Canada, June 8 – 11, 2026

Geothermal Production via Balanced Circulation in Sandstone Aquifers – Where do the Cold Fluids go?

L. Buijze[1]*, E. Peters[1], H. Veldkamp[1], E. Calignano[1], H. van Oeveren[2], J. Reijs[3] and A. Vondrak[2]
Geological Survey of the Netherlands, TNO, Utrecht, the Netherlands[1]*, Ennatuurlijk Aardwarmte, Middenmeer, the Netherlands[2], Gaia Energy, Schiphol, the Netherlands[3]
Corresponding author (*) loes.buijze@tno.nl

Keywords: sandstone aquifer, cooling, geomechanics, seismicity

ABSTRACT

Geothermal heat in the Netherlands is produced via balanced circulation between two or more wells in porous sandstone reservoirs at depths of 1.5 – 3 km. After heat is extracted at the surface, the cooled brine is reinjected which will progressively cool the reservoir. Knowledge of how this cooling evolves in space and time is important as it impacts the boundaries of the geothermal license area, project lifetime assessment, as well as fault reactivation, and seismic hazard- and caprock integrity assessment. In turn, these assessments guide limits on injection pressures and temperatures, and hence extracted heat and revenue. Simplified predictive models are routinely used to forecast cooling of the rock volume around the geothermal reinjection well with time. However, since field validation of such models was lacking there are substantial uncertainties in these models. Recently, several replacement geothermal wells were drilled close to former injection wells. This provided a unique opportunity to probe the cooled reservoir rock in the vicinity of the injector. Here, we present various observations and temperature logs acquired in these wells at different geothermal sites within the TKI Geo4All research program. The observations showed that 1) cooling was less than expected from the models, and 2) cooling was far from uniform over the reservoir interval. Possible mechanisms behind the observed cooling profiles were modeled, including the effect of facies and heterogeneity on flow, and density-driven flow. The heterogeneous cooling is expected to have significant impact on, amongst others, the seismic hazard calculations and caprock integrity assessment.

1 INTRODUCTION

In the Netherlands, deep geothermal heat is produced mainly from permeable sedimentary formations, notably sandstone reservoirs of Jurassic/Cretaceous or Permian Age at depths of 1.5 – 3 km and temperatures up to 100 °C (e.g. Mijnlieff, 2020). The first deep geothermal project in the Netherlands was developed in 2007, and since then the number of projects has grown to 23 operational projects in 2024 (Ministry of Climate and Green Growth, 2024). Geothermal production occurs via balanced circulation of fluids between two or more wells at relatively small overpressures, without hydraulic stimulation. After heat is extracted at the surface, the cooled brine is reinjected at temperature of 35 °C or lower, resulting in a temperature difference ΔT of several 10's of °C with respect to the initial reservoir temperature. The reinjection of cold brines is expected to cool down the reservoir around the injection well over time, eventually leading to thermal breakthrough at the production well. Knowing how this cooling progresses in space and time is important for a variety of reasons: for forecasting the geothermal potential (e.g. TNO, 2016) and the chance of exceeding the license boundary, and for (mandatory) seismic hazard and risk assessment (SHRA) (TNO-AGE & EBN, 2023, Fokker et al., 2023) and caprock stability assessment (Mijnlieff & Maaijwee, 2023). These forecasts in turn guide limitations on injection pressures and temperatures, and hence on heat produced and project revenue. However, models to predict cooling are often simplified, assuming for example uniform reservoir properties, and field data to validate these models is lacking, which may lead to overly conservative or uncertain forecasts. A combination of model improvements and field data is needed to reduce uncertainties on doublet lifetime estimates and safe ranges of injection pressures and temperature.

In this article new temperature measurements probing cooled reservoir intervals measurements at two geothermal projects (Bleiswijk Geothermie and Middenmeer Geothermie) are presented. These measurements were taken in replacement wells drilled in parallel trajectories to former injection wells which had been operational for 10 years but had to be taken out of commission due to e.g. corrosion issues. At the reservoir level, the distance between the replacement injections wells and old injectors was 80 – 200 m, which is nearby enough to expect significant cooling to be visible. The measurements provide a unique opportunity to check and validate models forecasting cooling. The observed temperatures are interpreted with the help of simplified reservoir modeling evaluating the effect of heterogeneity, completion and temperature dependent density. The outcomes are compared to the 'default' models for SHRA and caprock integrity used in the policy domain.

2 BLEISWIJK CASE STUDY

The Bleiswijk 1b Geothermie project (production license: Bleiswijk 1b) is one of two geothermal projects near Bleiswijk, in the southwest of the Netherlands, and is currently operated by Gaia Energy on behalf of IPS Geothermal. Initially the project consisted of two of the oldest geothermal wells in the Netherlands, producer VDB-GT-03 and injector VDB-GT-04, which were both drilled in 2009. The wells targeted the Delft Sandstone Member of the Schieland Group (NB: initially listed as Rijswijk Sandstone Member, but later reinterpreted as Delft Sandstone Member), which is overlain by the Rodenrijs Claystone Member and underlain by the low net-to-gross Alblasserdam Member. The top depth of the Delft Sandstone Member is 1815 m TVD at VDB-GT-03 and 1758 m TVD at VDB-GT-04 (Figure 1). Injection occurred over a gross reservoir height of 57 m. Production started in 01-2010, at average production rates of 111 m^3/hr, maximum production rates of 150 m^3/hr, production temperature of 65°C, an average reinjection temperature of 24°C, and a maximum injection pressure of 30 bar. From 2010-2019 the cumulative brine volume circulated was $8.7 \cdot 10^6$ m^3, and heat produced was 1.06 PJ. Due to integrity issues in VDB-GT-03 production was stopped in 2019, and the well was partially abandoned at a depth of 730 mMD. In 2024 the two replacement wells VDB-GT-05 (producer) and VDB-GT-06 (injector) were drilled. During drilling a larger reservoir thickness than initially thought amounting to of 220 m gross. Hence, VDB-GT-05/06 were completed to greater depths than VDB-GT-03/04. Injection in VDB-GT-06 is projected to start in Q1 2026. The horizontal distance between VDB-GT-04 and VDB-GT-06 is 60 (top) to 160 (VDB-GT-04 TD) m.

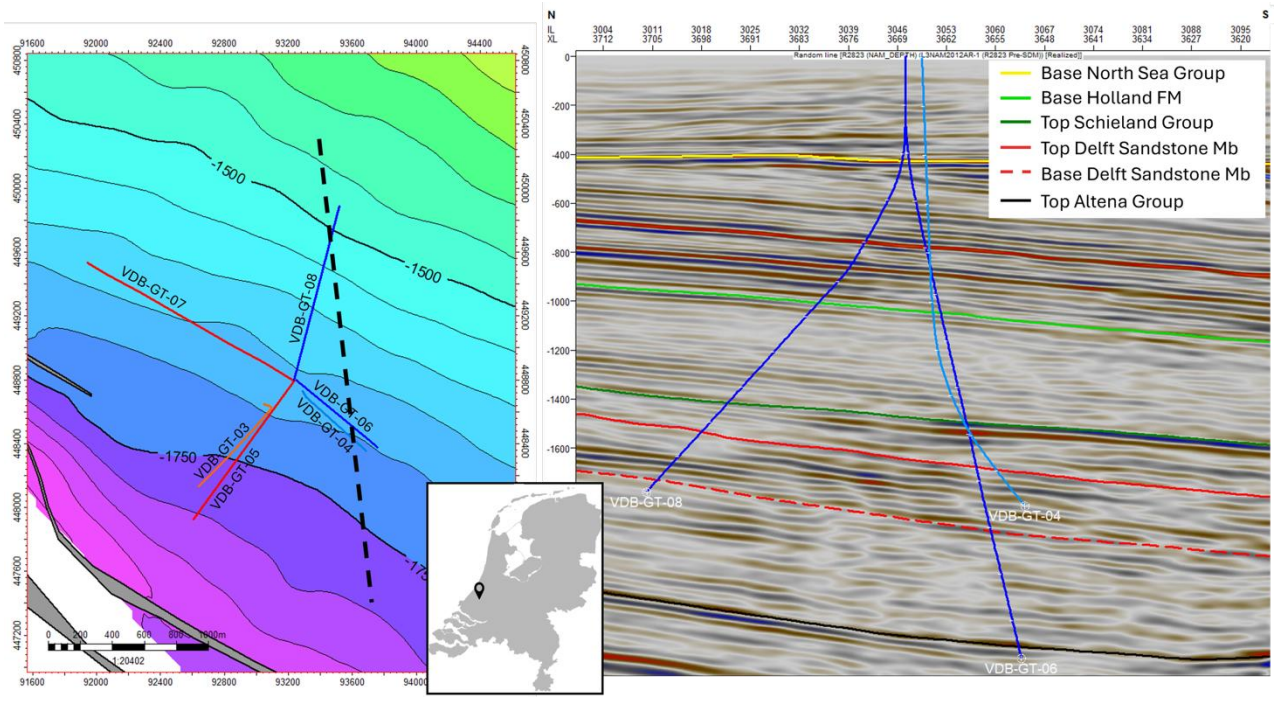


Figure 1. Overview of the Bleiswijk 1b Geothermie project.

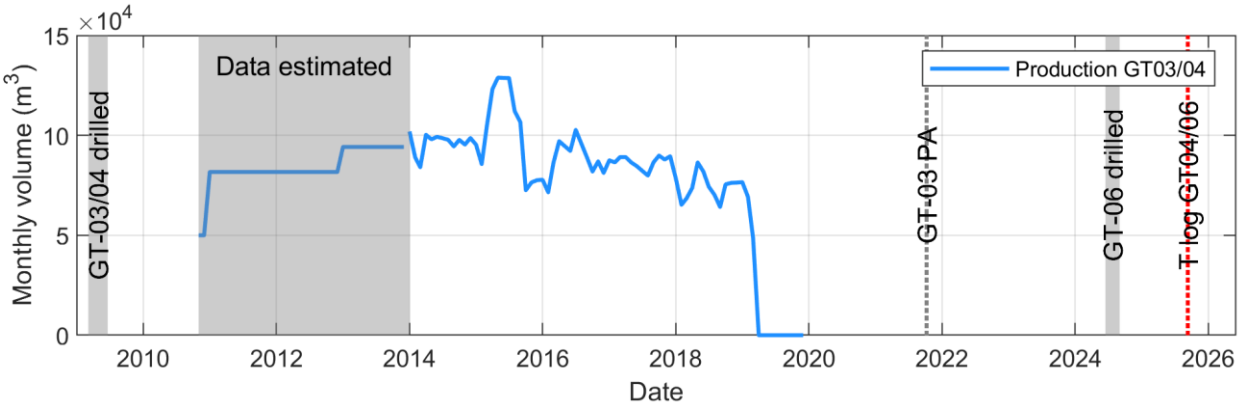


Figure 2. Production history of VDB-GT-03/04 and timing of drilling of VDB-GT-05/06 and temperature logging.

2.1 Bleiswijk temperature logging

Dedicated pressure and temperature logs were run in the completed wells VDB-GT-04 (old injector) and VDB-GT-06 (new injector) in September 2025. This was 6.5 years after injector in VDB-GT-04 was stopped, and ±1 year after drilling and testing of VDB-GT-06 (Figure 2). The temperature measurement is thus expected to reflect a stabilized temperature profile, unperturbed by the drilling. A 0.75" piezo memory pressure and temperature gauge was deployed on slickline cable. The accuracy of the pressure measurement was <0.1 bar and the accuracy of the temperature reading was <0.5°C. The run-in was done at speeds up to 50 m/min. Upon reaching the maximum logging depths of 1881 mMD (VDB-GT-04) and 2020 mMD (VDB-GT-06), the gauge was left to equilibrate for 15 minutes. Subsequently, the gauge was run up at slower speeds of 10 m/min to allow for temperature equilibration of the gauge. The temperature data shown here are from the upgoing tracks.

2.2 Modeling of cooling at Bleiswijk

To explain the driving mechanisms behind the observed cooling profiles simplified flow model simulations were done. A model was created in which the geometry was simplified to a rectangular shape with three main units: overburden, reservoir and underburden. The model includes an injection well and a production well. This model geometry is close to what is simulated in simplified flow model tools used in the regulatory domain (e.g. Fokker et al. 2023). The top and bottom surface of the reservoir were based on the well tops, thus taking into account the dip of the reservoir between the two wells. In a sensitivity analysis the effect of reservoir heterogeneity on cooling was assessed in a simplified manner. The thermo-hydraulic simulations were done using industry standard simulator Eclipse. For most cases, the thermal simulation was simplified, with the flow and heat solved with a simplified coupling. Only the changes in viscosity due to temperature were included. For the simulations to investigate the density-driven flow, a coupled thermo-hydraulic simulation was run. To isolate the impact of the density, two simulations were done with this simulator with and without variability in the density. The simulations without variability in the density were done by reducing the thermal expansion coefficients which describe the variation in density with temperature.

Four cases were simulated:

Case 1 Homogeneous model: This model has homogeneous properties with three main layers (overburden, reservoir and underburden) and screens in the reservoir section as indicated on the well completion diagrams. The reservoir layer is ~55 m thick with a dip of 3°. To investigate the impact of temperature-dependent density of the brine on the flow, Case 1 was simulated with and without density-driven flow.

Case 2 Heterogenous model: Heterogeneity in flow properties is included both in the reservoir and the over- and underburden. This model is thicker than the model used in Case 1 to include a larger part of the over- and underburden because more flow is expected in the over- and underburden in this case. The heterogeneity was included by simulating a simplified facies distribution (sand and clay) based on the lithology recording in wells VDB-GT-03 and -04. For Case 2, we predicted the lithological properties at the location of VDB-GT-06 based on VDB-GT-03 and -04 only, to represent the prediction of the temperature prior to drilling. The facies distribution was simulated with sequential indicator simulation with the fractions of sand and clay based on the well logs and variogram ranges of 800 m, 800 m and 20 m in the major, minor and vertical direction.

Case 3 Heterogenous model with flow behind the casing: In the Case 2 heterogeneous model, the possibility for flow behind the casing is included, which is possible because the annulus behind the deepest casing is not cemented or closed off by a packer below 921 mMD.

Case 4 Heterogenous model with lithology of VDB-GT-06: Same model settings as Case 3 were used but now including the lithology logged in VDB-GT-06 in addition to the lithology at VDB-GT-03 and -04. The lithology for VDB-GT-06 was based on the Gamma Ray log (GR): GR < 50 gAPI is taken as the sandy facies. The cut-off is taken such that the sand/clay distribution is consistent with VDB-GT-04. This case was also simulated with and without density-driven flow.

For all cases, the length and width of the model is 2650 m by 1335 m and the grid cell size is 20 by 20 m. Constant pressure and temperature boundaries were imposed on all sides. For the simulations investigating the impact of density-driven flow, a constant pressure was applied to the lateral boundaries and at the top and bottom a thermal boundary condition based on Vinsome and Westerveld (1980) was implemented. The input properties common to all the flow simulations are summarized in Table 1. A summary of the properties for the 4 cases is presented in Table 2.

Table 1. Input settings for the flow simulations of Bleiswijk.

Parameter	Name	Unit	Value		Name	Unit	
VDB-GT-03 top & base screens (producer)		mMD (m TVDRT)	2022-2106 (1802-1863)	Initial temperature	T_0	°C	10 + 30 * zTVD
VDB-GT-04 top & base screens (injector)		mMD (m TVDRT)	1881 – 1998[a] (1746 – 1825)	Fluid density at standard condition	ρ_f	kg/m^3	1064.3
Well diameter	d_{well}	inch	8.5	Fluid heat capacity			3.73 (10 °C) 3.77 (60 °C) 3.8 (100 °C)
Injection temperature	T_{inj}	°C	25	Fluid salinity		ppm	90000
Injection rate	Q	m^3/hr	125	Injection pressure	P_{inj}	bar	182 (1800 m)

[a] For Cases 3 and 4 flow behind the casing is possible from 921 mMD.

Table 2. Input settings Bleiswijk for cases 1 to 4

			Case 1			Cases 2 – 4	
Parameter	Name	Unit	overburden	reservoir	under burden	sand	shale
Thickness	H	M	100	53-55	100	350 m overburden, 50-60 m reservoir, 150 m underburden	
Number of layers	n	-	6	20	6	30 overburden, 10 reservoir, 15 underburden	
porosity	ϕ	-	0.05	0.2	0.05	0.2	0.12
Net/gross	NG	-	0.2	0.8	0.2	0.8	0.3
Horizontal Permeability	kh	mD	1	300	1	300	5
Vertical permeability	kz	mD	0.001	10	0.001	10	0.01
Thermal conductivity (rock + fluids)	T	kJ/m/day/K	240	280	240	260	260
Rock Heat capacity		kJ/m^3/K	2700	2700	2700	2700	2700

2.3 Results

Figure 3 shows the observed and simulated temperature at the newly drilled well VDB-GT-06. A clear temperature low down to 44°C was observed at 1800 m TVD, a clear indication of the cold front related to injection in VDB-GT-04. The observed temperature was a decrease of ~20°C with respect to the initial reservoir temperature, but 18 °C higher than the injection temperature in VDB-GT-04. The amount of cooling gradually reduced towards the top and bottom of the reservoir, propagating into the over- and underburden. Also, somewhat higher in the overburden at 1650 m TVD some cooling was observed.

The simulated temperature is shown for all four cases at the end of the simulation period (September 2025) when the temperature was logged. The simulated temperature at the location of VDB-GT-06 for Case 1 shows the traditional cooling in the reservoir and cooling in the over- and underburden. The lowest simulated temperature in the reservoir is 31°C, which has increased from the minimum temperature of 26°C that was simulated directly after the injection stop in 2018. This is much lower than the observed temperature of 44°C.

In case heterogeneity in the reservoir properties is included (Case 2), the results do not change much. The average properties are very similar to the homogeneous model and in the reservoir, mainly sand is simulated, resulting in very similar temperatures at VDB-GT-06. Since VDB-GT-06 is behind the cold front, variability in the front is not well observed with VDB-GT-06. In addition, due to the period of 6 years without flow, the front has become smooth due to thermal conduction both in the horizontal and the vertical direction.

In Case 3, the impact of the flow behind the casing in VDB-GT-03 is well visible. Some of the cold water is injected above the reservoir and the temperature in the main reservoir section is 1 degree higher. VDB-GT-06 is still well within the cold-water bubble. The reduced temperature above the reservoir is now better reproduced although the exact depths of the main cooling was not well represented.

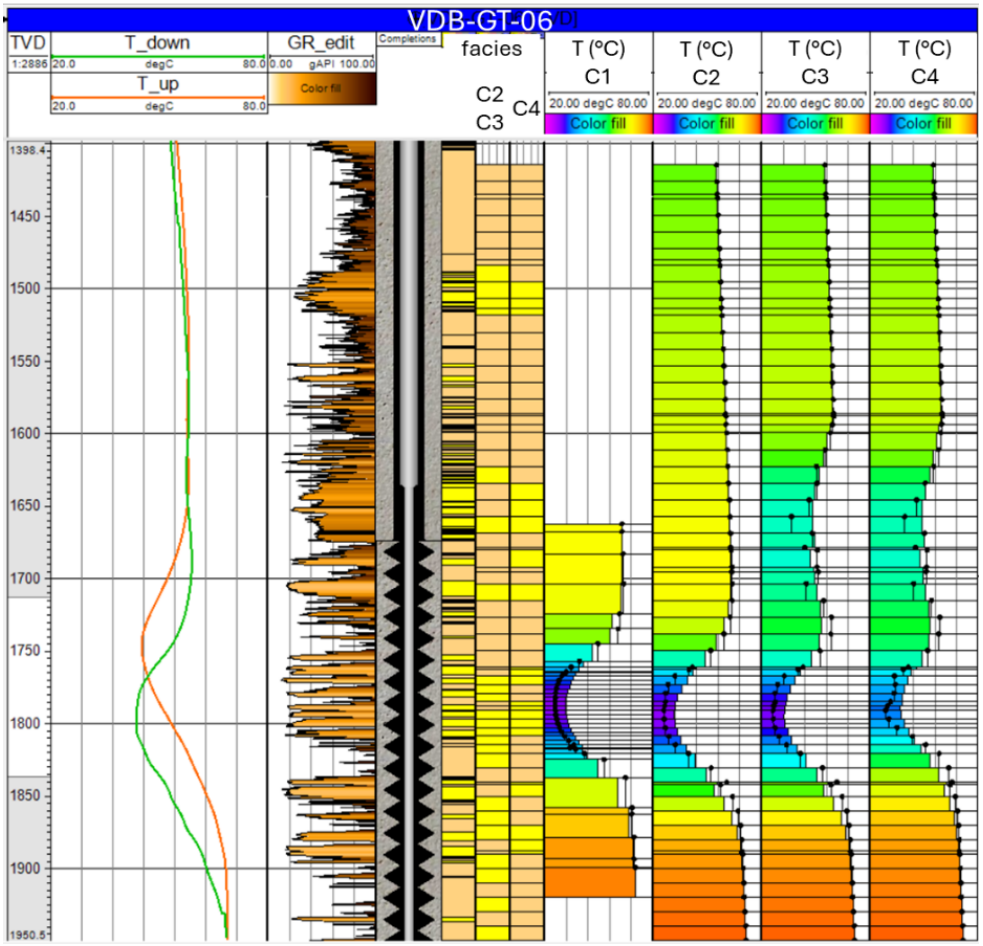


Figure 3. Well section for VDB-GT-06 showing the tracks: observed temperature (red: up and green: down), GR (scaled between 0 and 100 gAPI), completion, facies (facies from GR, simulated facies based in VDB-GT-03 and 04 only, simulated facies based in VDB-GT-03,04 and 06; yellow is sand, orange is clay/mixed), simulated temperature at the end of injection (black dots and lines) and at the end of the simulation period (September 2025) for Cases 1 to 4 (colored profiles).

In the final case (Case 4, the last track in Figure 3), the observed lithology derived from VDB-GT-06 was included in the facies simulation. In the previous cases, the lithology at the location of VDB-GT-06 was based on VDB-GT-04 only. In this case the temperature in the main reservoir section in VDB-GT-06 was closer to the observed temperature, because the connectivity between the wells was reduced due to incorporation of the lithologies of all three wells. The simulated temperature is however still lower than the observed temperature. Better fits to the observed data could probably be obtained by matching the permeability in detail based on the observations, however that is beyond the scope of the current study.

The impact of the density-driven flow has been analyzed in Cases 1 and 4 by running with constant density and temperature-dependent density. The differences between the runs were very small. To see more effect of the differences in density, the run was continued for another 25 years to 2045 (without production or injection). Over this long period some differences were seen but never more than 0.5°C. No displacement of the bubble of cold water in down-dip direction was observed. The dip in this model is modest however (57 m height difference between the wells which are ~1 km apart resulting in a dip of ~3°). Some sinking of the bubble is visible either as more temperature decrease in the bottom part of the cold bubble or as reduced temperature recovery in the bottom part of the reservoir for the case with density-driven flow.

3 MIDDENMEER GEOTHERMIE

The Middenmeer Geothermie project is situated in the northwest of the Netherlands and is currently operated by Ennatuurlijk Aardwarmte. The project consists of four doublets. The doublet of interest for this study is Doublet #2 which is composed of injector MDM-GT-03-S1 and producer MDM-GT-04, which were drilled in 2013-2014. The wells target the Slochteren Sandstone Formation (Permian age), which is capped by Zechstein 1 Formation (Permian age) which is at its base comprised of anhydrites and carbonates. The reservoir is underlain

by mudstone, silts and sands of the Ruurlo Formation (Carboniferous age). The top reservoir in MDM-GT-03-S1 was encountered at 2250 m TVDSS (2474 mMD), and at 2156 m TVDSS (2394 mMD) in MDM-GT-04, and the gross thickness of the reservoir is ~210 m. Production from Doublet #2 lasted from November 2014 to November 2024, at average production rates of 136 m^3/hr, maximum production rates of ~250 m^3/hr, production temperature of 92°C, an average reinjection temperature of 35 °C, and a maximum injection pressure of 56.5 bar. A total of $1.2 \cdot 10^7$ m^3 of brine was reinjected. In 2024-2025 wells MDM-GT-07-S2 and MDM-GT-11-S2 were drilled to replace respectively the wells MDM-GT-04 and MDM-GT-03-S1 of Doublet #2. At the reservoir depth, the horizontal distance between the former injector and the new injector is 120 at the top and 220 m at the bottom of the reservoir.

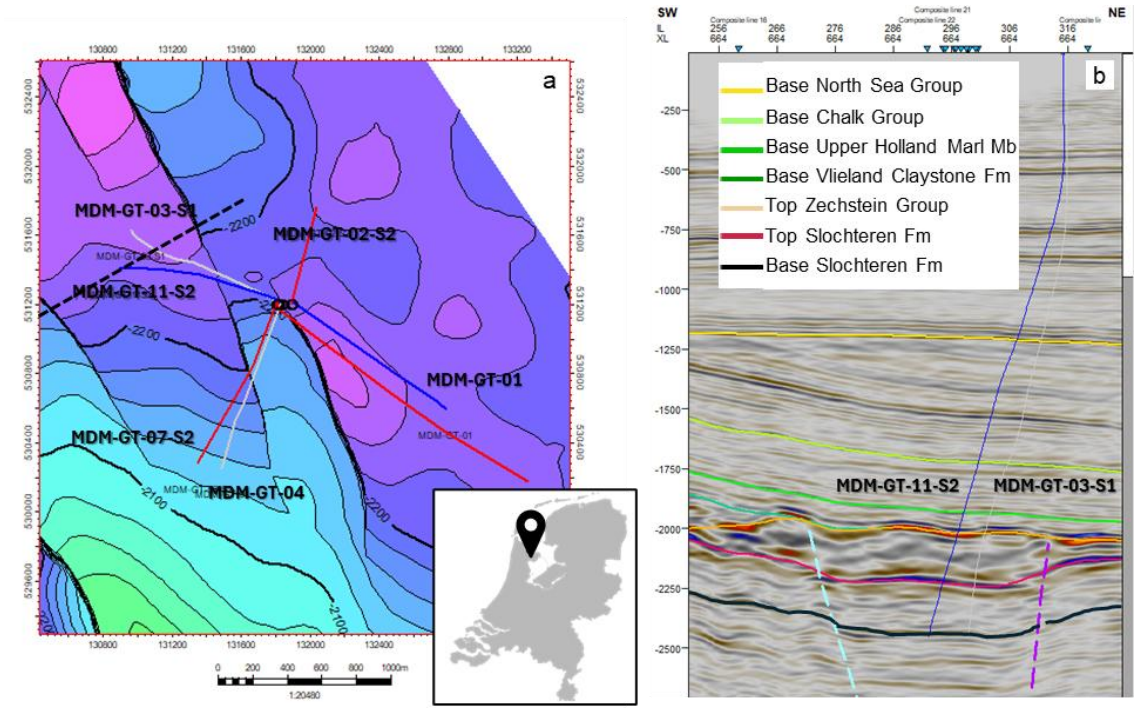


Figure 4. Overview of the Middenmeer project area of interest (from Buijze et al., 2025). a) Map view of wells in the Middenmeer I and II license areas (exc. MDM-GT-05 which is just to the north of the map). The colours indicate the top of the Slochteren Formation. b) SW-NE vertical cross-section (see dotted line in Figure 1a for the location). Gray: former injection well MDM-GT-03-S1, blue: new injection well MDM-GT-11-S2.

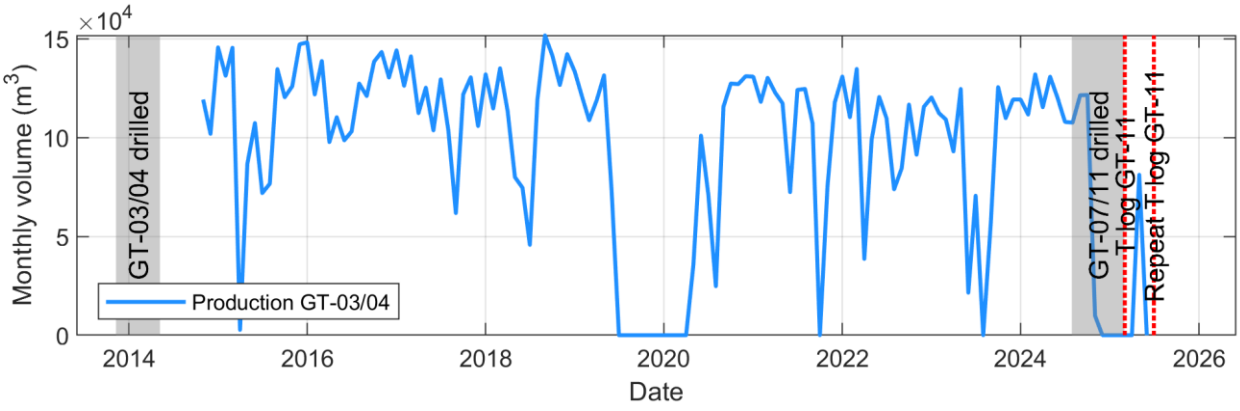


Figure 5. Production showing MDM-GT-03/04, drilling MDM-GT-11-S2 and timing of temperature logs.

3.1 Middenmeer temperature logging

Multiple temperature measurements were done in MDM-GT-11-S2 (new injector). The first data were recorded with temperature sensors on logging tools deployed in three separate log runs 1-3 days after drilling of the final section was completed (Buijze et al., 2025; runs 1 and 2 in Figure 6). These logs were done over the open hole reservoir section, before completion of the well. Another dedicated temperature log was run in June 2026, 3 months after drilling was completed and 1 month after well testing in nearby injector MDM-GT-03-S1 (Figure 5 and run 4 on the first track in Figure 6). This log was done using a memory PT gauge deployed on slickline, with

an accuracy of <0.5 °C. The gauge was run down and up the well once at velocities up to 30 m/min. The run-down and run-up velocities were reduced to 3 m/min over the interval 2432 – 2664 mMD covering the reservoir.

3.2 Modeling of cooling at Middenmeer

The model approach for the Middenmeer case study was similar to that at Bleiswijk (Section 2.2) The reservoir thickness in the generic Middenmeer model was 200 m thick with a dip of 4°. The total model dimension was 3400 x 1500 m, gridded in 15 x15 m cells and aligned with the faults in the area (Figure 4). The vertical resolution varied between the overburden, reservoir and underburden. Boundary conditions were taken as constant pressure and temperature on the top and bottom boundaries and on the short sides of the rectangle. The long sides of the model are assumed no flow boundaries because of the presence of faults. Three cases were simulated:

Case 1 Homogeneous model: base case with homogeneous properties, three main layers (overburden, reservoir and underburden) and screens in the reservoir section as indicated on the well completion diagrams. As for the Bleiswijk case, Case 1 is simulated with and without density-driven flow.

Case 2 Heterogeneous model: This case is the same setup as case 1, but the N/G is modelled in the reservoir part based on the observed well logs. The N/G was modeled using Gaussian random function simulation with variogram settings of 1000 m, 1000 m and 20 m in the major, minor and vertical direction. The distribution is based on the well logs. The N/G logs are derived from the normalized GR logs: the GR logs are normalized between 0 and 130 gAPI. Reservoir is defined as a GR lower than 85 gAPI. This results in an average N/G at the wells of 0.7, which is in line with the homogeneous model.

Case 3 Heterogeneous model with higher perm zone: In this case, the reservoir is split into two zones: the lower 60 m is dune facies with better permeability than the upper part of the reservoir. The N/G is simulated separately for the two reservoir zones, as for Case 2. The vertical permeability is made dependent on the N/G.

Table 3. Input settings for the flow simulation of Middenmeer.

Parameter	Name	Unit	Value	Parameter	Name	Unit	
MDM-GT-03-S1 top & base screens (injector)		mMD (mTVD)	2474-2686 (2249-2431)	Initial temperature	T_0	°C	10 + 36 * zTVD
MDM-GT-04 top & base screens (producer)		mMD (mTVD)	2394 – 2637 (2156-2366)	Fluid density at standard condition	ρ_f	kg/m^3	1110.2
Well diameter	d_{well}	inch	7.5	Fluid heat capacity		kJ/kg/K	3.5 (10 °C) 3.54 (60 °C) 3.57 (100 °C)
Injection temperature	T_{inj}	°C	35	Fluid salinity	s	ppm	150000
Injection rate	Q	m^3/hr	130	Injection pressure	P_{inj}	bar	182 (1800 m)

Table 4. Input settings Bleiswijk for the Case 1 and sensitivity analyses Case 2 – 4.

Parameter	Name	Unit	Overburden	Underburden	Reservoir		
					Case 1	Case 2	Case 3
Thickness	H	m	150	100	180-210	180-210	180-210
Number of layers	n	-	10	7	40	40	40
Porosity	ϕ	-	0.01*	0.05	0.12	0.12	0.12
Net/gross	NG	-	0.1	0.1	0.7	Modeled	Modeled
Horizontal Permeability	kh	mD	0**	0.001	120	120	Upper: 70 mD Lower 60 m: 170 mD
Vertical permeability	kz	mD	0**	0.00002	2.4 (0.02*kh)	2.4 (0.02*kh)	NG>0.7: 0.01*kh NG<=0.7: 0.1*kh
Thermal conductivity (rock + fluids)	T	kJ/m/day/K	340	240	280	280	280
Rock Heat capacity		kJ/m^3/K	2700	2700	2700	2700	2700

* Although the Zechstein anhydrite above the Slochteren does not have porosity, for practical purposes a porosity is used in the simulation model. This pore volume is not connected to the reservoir because there is no permeability.

** At the bottom of the Zechstein anhydrite, is a claystone layer of a few m thick, which is modelled with the same settings as the shaly underburden (kh = 0.001 mD and kz = 0.00002 mD).

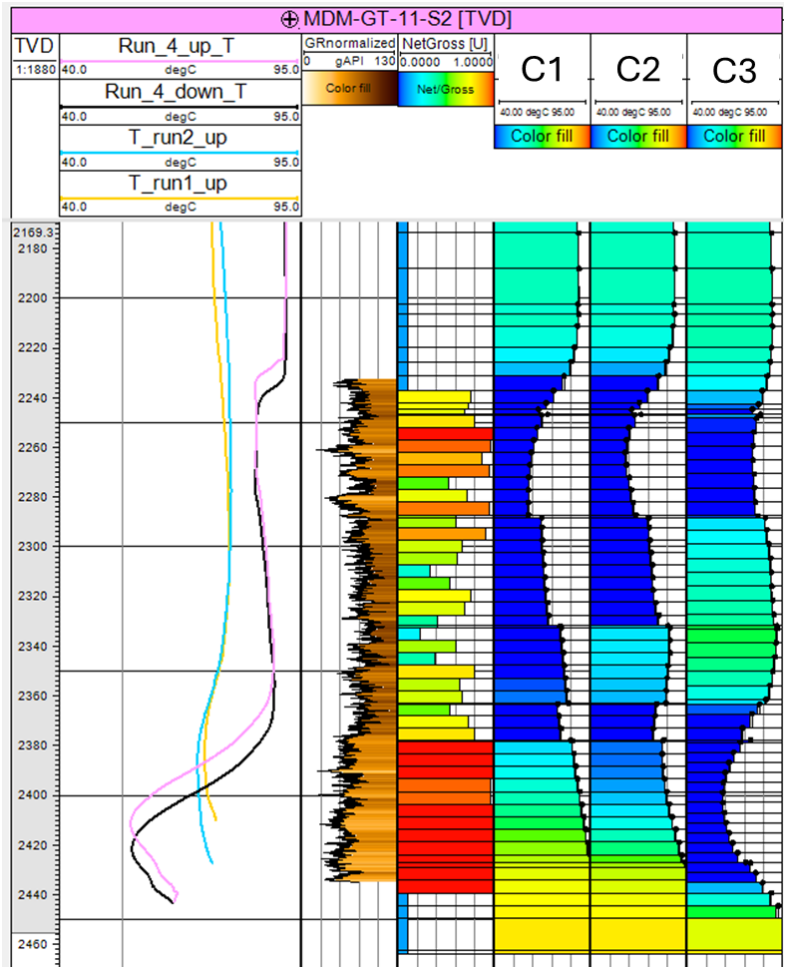


Figure 6. Well section for MDM-GT-11-S2 showing the tracks: observed temperature, GR (scaled between 0 and 130 gAPI), upscaled N/G, simulated temperature at the end of the injection period (Nov 2024, black dots and lines) and at the end of the simulation period (May 2025, colors) for Cases 1 to 3.

3.3 Results

The results show that the reservoir interval has been cooled with respect to the initial reservoir temperature (94°C), but also that cooling was not uniform with depth (Figure 6, first track). The temperature at the base of the Zechstein caprock was 90°C, dropping to 80°C over the top 50 m of the reservoir indicating 10-15 °C of cooling. Between 2475 – 2575 mMD, the temperature increased near-linearly to 85°C. Below 2575 mMD the temperature decreased, reaching a minimum of 52°C at 2525 mMD. Temperature increased again to 60°C near the base of the reservoir. Hence, most cooling was observed in the bottom third of the reservoir. However, the minimum recorded temperature of 52°C was still above the injection temperature of ~35°C in the nearby (<200 m) injector well MDM-GT-03-S1. The main cooling is associated with the high net-to-gross interval near the base of the reservoir. A correlation with a more extensive log suite presented in Buijze et al. (2025) showed the dominant cooling to be linked to higher porosity interval although the correlation was not obvious everywhere.

In the homogeneous model (Case 1), the match with the observed temperature in MDM-GT-11-S2 is not very good (Figure 6, track C1). The observed cooling is much stronger in the bottom than in the top, whereas in the simulations cooling is stronger near the top of the reservoir. This is mainly caused by the distance of MDM-GT-11-S2 with respect to MDM-GT-03-S1, which is a bit further away from MDM-GT-03-S1 at the bottom of the reservoir than at the top. The difference between the end of the injection period (black dots an lines, Nov 2024) and the simulations (May 2025) is short and has little impact in Middenmeer. For Case 2 (Figure 6, track C2), the distribution of the N/G is simulated based on the well logs. This results in a bit more cooling in the bottom of the well, but there are no major changes. When the difference in upper and lower reservoir is added in Case 3, the results change considerably. In Case 3 (Figure 6, track C3), the main cooling occurs in the high permeability bottom part of the reservoir. In the top only a moderate amount of cooling occurs in the model (to 77°C), similar to the observations. By further adjusting the permeability, a more detailed match to the temperature log could be created but this is beyond the scope of the current work. The results clearly show that including more detailed knowledge of the reservoir and heterogeneity improved the simulated distribution of the cold bubble. The lower

position of the cold water means in this case, that the cooling on the seal is much lower than for a homogeneous distribution, both in the values reached and the extent (Figure 6).

As for the Bleiswijk case study, for this model the impact of the density-driven flow was simulated and the conclusions were the same as before. The impact of the variability in temperature is small (less than 1°C).

4 DISCUSSION

4.1 Mechanisms for vertically heterogeneous cooling

The observations of temperature in VDB-GT-11 and MDM-GT-06-S2 show that the temperature distribution can be considerably more complex than the simple, homogeneous models predict. The simulations show that variability in permeability can explain a large part of the variability. However, in the Bleiswijk case, including the details of the completion proved important. Based on the current simulations, the cooling in the seal is caused by a combination of flow behind the casing and permeable layers within the seal. The cooling above the reservoir would likely have been a lot smaller if the casing had been cemented (or closed-off by a packer) and the fluids had been injected in the reservoir only, as is the well standard design that is used today.

In this analysis only some of the aspects that influence the distribution of the cold fluids have been analysed. Other factors that can strongly influence the distribution are for example the boundary conditions: sealing or open faults, or the presence of a depleted oil or gas field can influence the direction in which the fluids flow. Also the presence of other doublets/wells in the vicinity will influence the flow. Investigating these aspects was beyond the scope of this study. Furthermore, the properties were estimated in a simplified way without including all the log data, in particular for the Middenmeer case study. Also, hard cut-off values were used to model sand versus clay. For a detailed analysis of the reservoir cooling, other log information should be included in the analysis.

Please note that the facies for VDB and the N/G for MDM were simulated rather than interpolated. This means that the results depend on the seed used for the property simulation. Interpolation would result in one deterministic case, but results in overly smooth properties, which is less realistic. Simulating a full ensemble instead of a single realization would solve this but is beyond the scope of the current study.

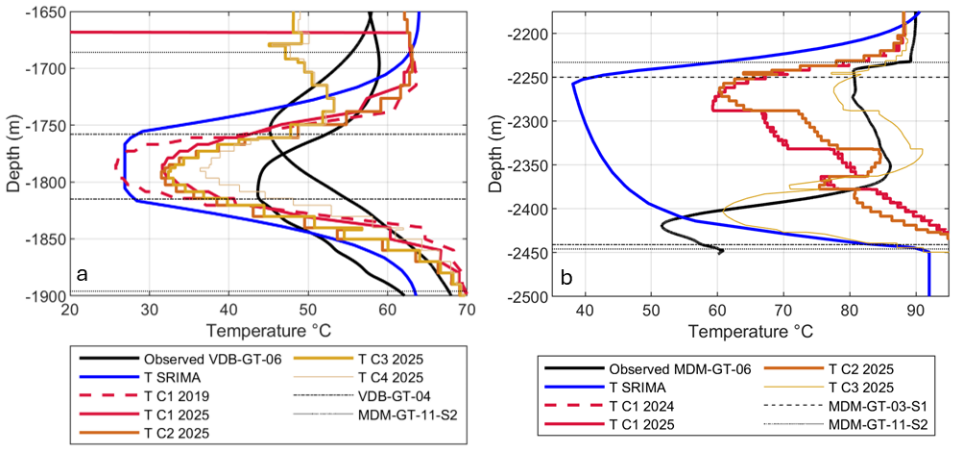


Figure 7 Comparison of observed temperature (black line), modeled temperatures (T C1-C4) and temperature modeled with SRIMA for the C1 input parameters. a) Bleiswijk, at 120 m from the injection well, b) Middenmeer, at 120 (top reservoir) to 220 (base reservoir) m from the injection well.

4.2 Implications

Within the regulatory framework for geothermal projects in the Netherlands the SRIMA tool is used to model pressure and temperature changes, stress changes in the reservoir, and the potential for fault reactivation and caprock fracturing. This aids in settings operational constraints in terms of maximum allowable injection pressure and minimum injection temperature. SRIMA a.o. relies on the assumptions of convective flow in the reservoir, and vertical conduction to the seal and base. The temperature computed with SRIMA is plotted together with the modeled temperature of Sections 2 and 3, as well as the observed temperature from the logs, at a distance from the injector (Figure 7). The comparison shows that the SRIMA temperature estimate was always (significantly) lower than the modeled and also the observed temperatures. The observed temperature profile and the profile modeled in Eclipse were more smoothed than that computed in SRIMA, reflecting the role

of conduction in the reservoir which is not included in SRIMA. Also, the temperature profile in SRIMA is uniform in the reservoir, whereas the Middenmeer case study demonstrates cooling may be heterogeneous (Figure 7b). Clearly, the SRIMA assumptions may not provide an adequate description of temperature at a distance from the well. This causes the cooling of the seal and base to be overestimated, and thermo-elastic stressing and fault reactivation to be overestimated, placing an overly conservative limit on the allowable injection pressures and cooling. For caprock cooling, a more detailed analysis of cooling around the injector itself is recommended. In general, this study shows the great value of having temperature observations away from the injector for model verification, as many effects would not be visible near the injector itself. Based on the results, it is recommended to use more realistic modeling of cooling, in combination with field measurements, to better estimate the potential for caprock fracturing, fault reactivation and the associated limits on safe production.

5 CONCLUSIONS

This article presents measurements of temperature within a cooled geothermal reservoir, at a certain distance from a former injector at two different geothermal projects, the Bleiswijk Geothermie and Middenmeer Geothermie projects. This provides a valuable and unique opportunity to compare model results of cooling to the field data. The measured temperatures were compared to simplified box models of the geothermal doublets, including some sensitivity analysis accounting for heterogeneity, well completion, and temperature-dependent density. The results show that

- The observed cooling away from the injector is generally less than modeled.
- Simplified model assuming convection but not conduction in the reservoir overestimate cooling in the reservoir and in the seal and base.
- Cooling can be heterogeneous in the reservoir, due to permeability variations. This may lead to very limited cooling of the caprock as was observed at Middenmeer.
- Wellbore completions can have an important effect on cooling of the caprock.
- Some reheating of the reservoir and further cooling of the caprock occurs after injection stop due to thermal conduction (<8°C over 8 years).
- The effects of density-driven flow are very limited both during production and after production stop. There appears to be very limited vertical flow due to lower vertical permeability.

The effects of conduction and heterogeneity should be included in models for caprock stability and fault reactivation, as the outcomes will likely have a strong effect on the allowable injection temperature and pressure to remain with a safe operating window in terms of caprock integrity and fault reactivation.

ACKNOWLEDGEMENTS

This work was performed as part of the Geo4All Innovation project funded by TKI Nieuw Gas, RVO, Netherlands.

REFERENCES

Buijze, L., Pascarella, A., Calignano, E., van Oeveren, H. and Vondrak, A.: Heterogeneous geomechanical properties and cooling in a sandstone reservoir exploited for geothermal production. *Proceedings,* European Geothermal Congress 2025, 6 – 10 October, Zürich, Switzerland (2025).

Fokker, P. A., Buijze, L., & Pluymaekers, M. P. D.: SRIMA: Background Information of Python tool. TNO Technical Report nr. TNO2023_R11303. (2023)

Kestin, J., Khalifa, H.E. and Correla, R.J.: Tables of the dynamic and kinematic viscosity of aqueous NaCl solutions in the temperature range 20-150°C and the pressure range 0.1 – 35 MPa. *J. Phys. Chem. Ref. Data*, **10(1),** (1981).

Mijnlieff, H. F.: Introduction to the geothermal play and reservoir geology of the Netherlands. *Netherlands Journal of Geosciences*, **99,** (2020), **e2**.

Ministry of Climate and Green Growth: Delfstoffen en aardwarmte in Nederland: Jaarverslag 2024. Den Haag, 14 juli 2025. www.nlog.nl. (2024)

TNO (2016): DoubletCalc 2D v1.0. https://www.nlog.nl/en/nieuws/doubletcalc-2d-v10

TNO-AGE, & EBN. Seismische Dreigings- en Risicoanalyse voor aardwarmteprojecten in Nederland. Utrecht: TNO-AGE, EBN. Retrieved from: https://www.nlog.nl/sites/default/files/2023-11/20230922_hoofdrapport_sdra_aardwarmteprojecten_-_shra_for_geothermal_projects.pdf (2023)

Vinsome, P.K.W. and Westerveld, J. (1980): A simple method for predicting cap and base rock heat losses in thermal reservoir simulators, *J. of Canadian Petroleum Technology*, **19(3),** (1980), 87-90.